Ay124

Winter 2015-16

Galactic Stellar Populations II

20 January 2016

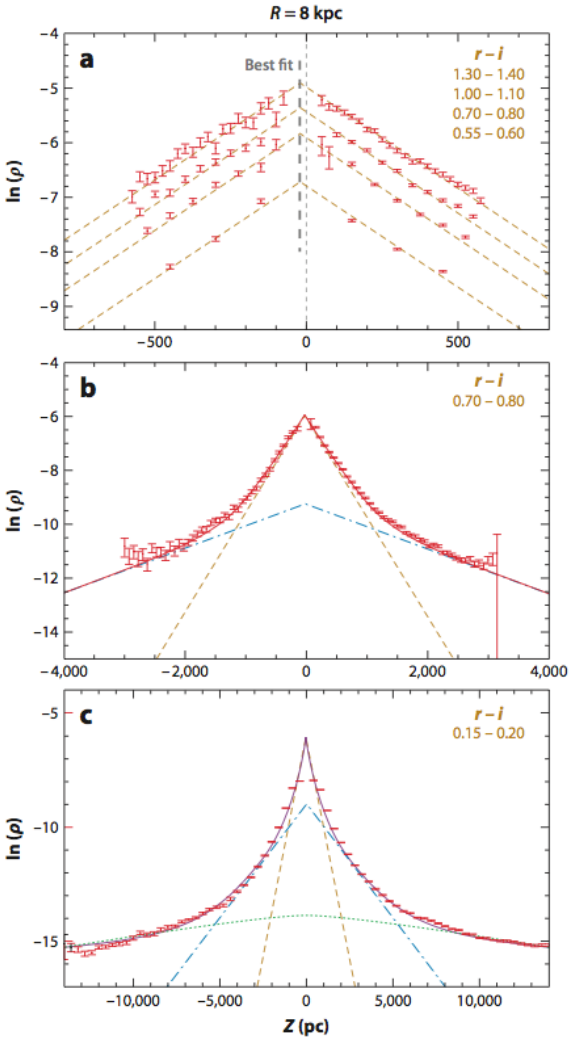

Figure 4

Cross sections through maps, similar to those shown in **Figure 3**, showing the vertical ($|Z|$) distribution at $R = 8$ kpc and for different $r - i$ color bins. The orange dashed lines are exponential models fitted to the red points (the sech^2 function is not a good fit; see footnote 28 of Jurić et al. 2008). The orange dashed lines in panel *a* correspond to a fit with a single, exponential disk. The vertical dashed line shows the best-fit position of the maximum density (not at 0 due to the Sun's offset from the disk midplane). The blue dot-dashed line in panel *b* corresponds to an additional disk component, and the data are fit with a sum of two disks with scale heights of 270 pc and 1,200 pc, respectively, and a relative normalization of 0.04 (the "thin" and the "thick" disks). The purple line in the bottom panel (closely following the data points) corresponds to a sum of two disks and a power-law spherical halo. The orange dashed line and the blue dot-dashed line are the disk contributions, and the halo contribution is shown by the green dotted line. For the best-fit parameters, see **Table 1**. Reprinted from Jurić et al. (2008).

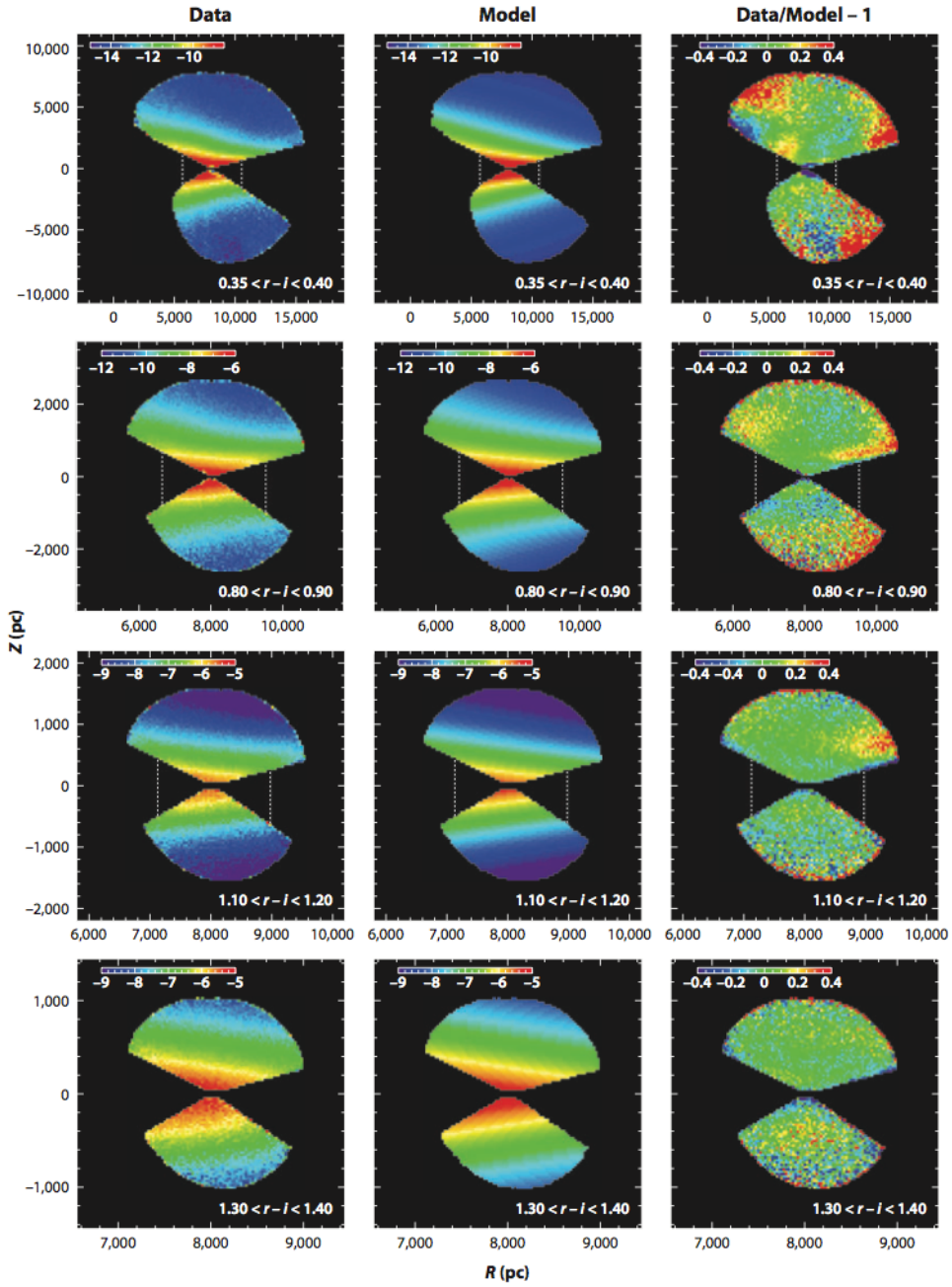

SDSS Color/Density Map of Galactic Main Sequence Stars

(from Ivezic et al 2012, ARAA)

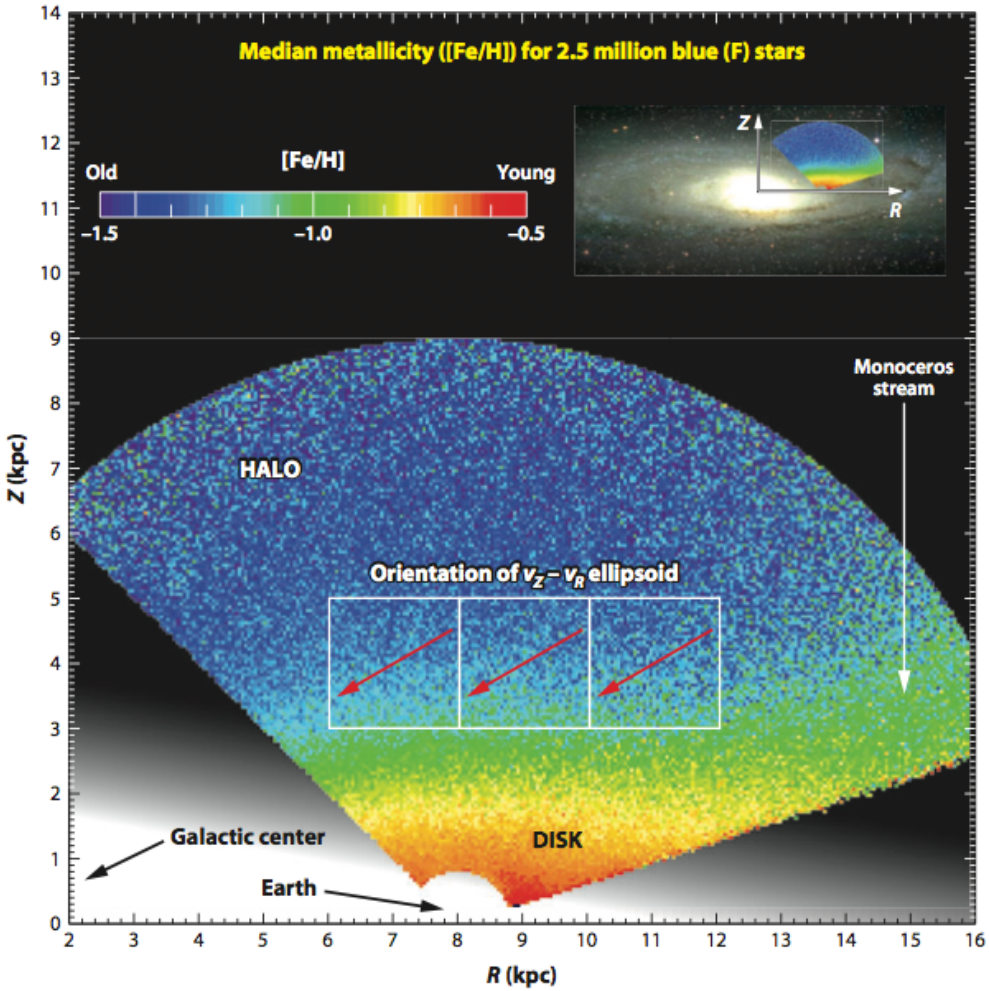

Figure 5

Variation of the median photometric stellar metallicity for ~2.5 million stars from the Sloan Digital Sky Survey with $14.5 < r < 20$ and $0.2 < g - r < 0.4$, and photometric distance in the 0.8–9 kpc range expressed in cylindrical Galactic coordinates R and $|Z|$. The ~40,000 pixels (50 pc by 50 pc) contained in this map are colored according to the legend in the top left. Note that the gradient of the median metallicity is essentially parallel to the $|Z|$ axis, except in the region of the Monoceros stream, as marked. The gray-scale background is the best-fit model for the stellar number-density distribution from Jurić et al. (2008). The inset in the top right illustrates the extent of the data volume relative to the rest of the Galaxy; the background image is the Andromeda galaxy. The three squares outline the regions used to construct the $v_Z - v_R$ ellipsoids shown in **Figure 16**. The arrows illustrate the variation of the ellipsoid orientation, which always points toward the Galactic center. Adapted from Ivezić et al. (2008a).

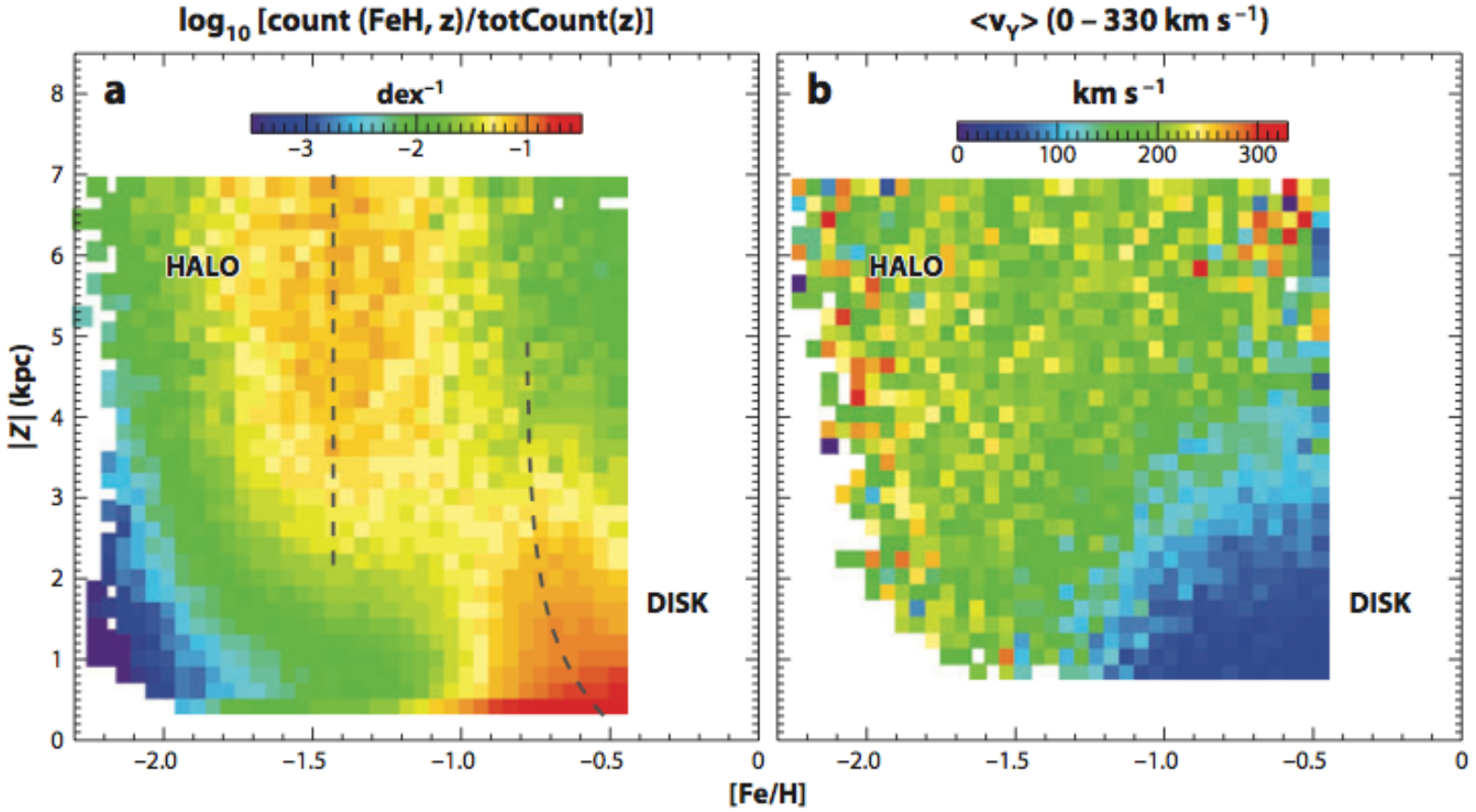

Figure 6

(*a*) The conditional metallicity probability distribution (each row of pixels integrates to unity) for ~60,000 stars from a cylinder perpendicular to the Galactic plane, centered on the Sun, and with a radius of 1 kpc. The values are color-coded on a logarithmic scale according to the legend on top. The lack of stars with $[Fe/H] > -5.0$ is due to a bias in Sloan Digital Sky Survey Data Release 6 reductions, and an updated version of this map based on Data Release 7 is shown in figure A.3 of Bond et al. (2010). (*b*) The median heliocentric rotational velocity component (the value of ~220 km s^{-1} corresponds to no rotation), as a function of metallicity and distance from the Galactic plane, for the ~40,000 stars from panel *a* that also satisfy $|b| > 80°$. Reprinted from Ivezić et al. (2008a).

$v_Z - v_R$ ellipsoids shown in **Figure 16**. The arrows illustrate the variation of the ellipsoid orientation, which always points toward the Galactic center. Adapted from Ivezić et al. (2008a).

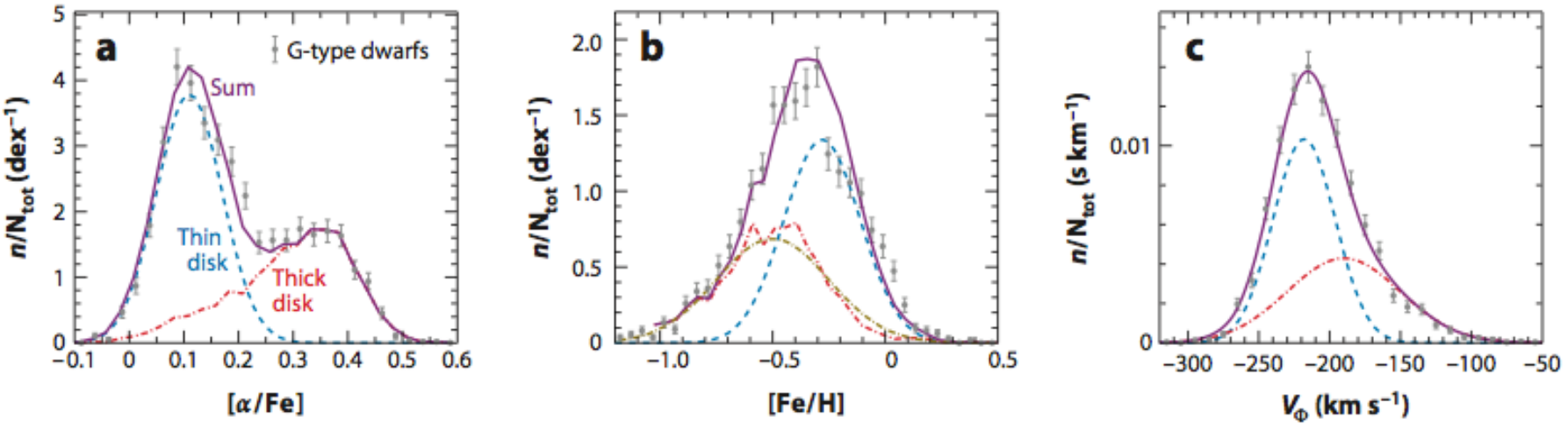

Figure 12

Tests of thin-/thick-disk decomposition using the sample of G-type dwarfs from Lee et al. (2011b). (*a*) The [α/*Fe*] distribution for ~2,300 stars in the fiducial bin $|Z| = 400$–600 pc as gray circle symbols with (Poissonian) error bars. The bimodality is easily seen. The observed distribution can be modeled as the sum (shown by the *purple solid line*) of two components: the [α/*Fe*] distribution for ~3,300 stars with $|Z| = 2$–3 kpc shifted to lower values by 0.03 dex (*red dot-dashed line*) and a Gaussian distribution, $N(0.11,0.06)$ (*blue dashed line*). The weights for the two components (0.43 and 0.57 for the thick and thin components, respectively) are consistent with a double-exponential fit to star counts. (*b*) The [*Fe/H*] distribution for the same stars from the fiducial $Z = 400$–600 pc bin as symbols with error bars. Similar to the [α/*Fe*] distribution, it can be modeled as the sum (purple solid line) of two components: the [*Fe/H*] distribution for stars with $|Z| = 2$–3 kpc shifted to higher values by 0.2 dex (*jagged red dot-dashed line*) and $N(-0.28,0.17)$ (*blue dashed line*). The weights for the two components (0.43 and 0.57) are the same as in panel *a*. The [*Fe/H*] distribution for stars with $|Z| = 2$–3 kpc is well described by $N(-0.50,0.25)$ (after application of a 0.2 dex offset), shown as the smooth dark yellow dot-dashed line. (*c*) The rotational velocity distribution for the same stars from the fiducial $|Z| = 400$–600 pc bin as symbols with error bars. It can be modeled as a linear combination of two Gaussian distributions, $N(-218,22)$ and $N(-190,40)$, again using the same relative weights (and line styles) as in panel *a*.

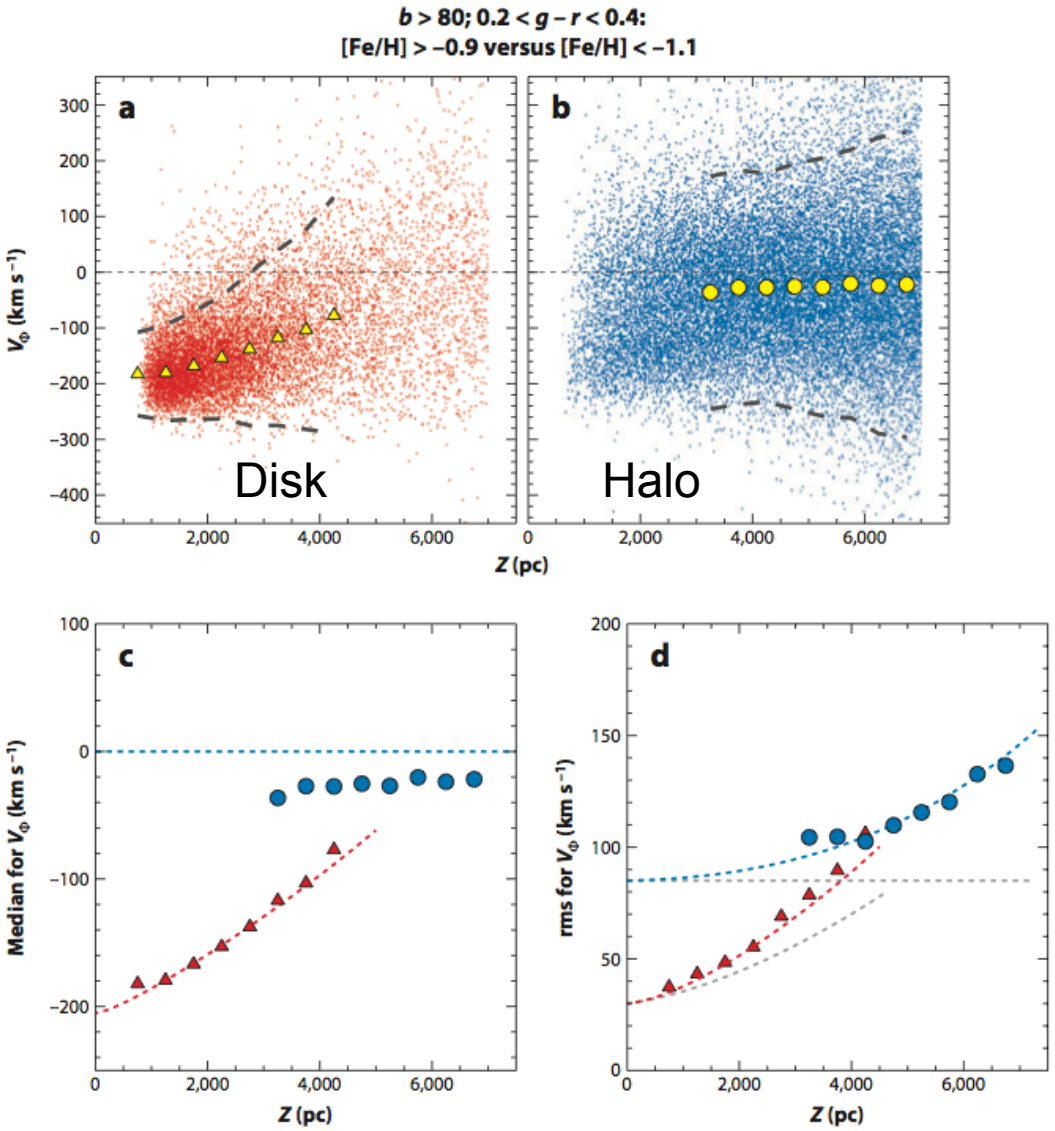

Figure 7

A comparison of the variation of rotational velocity (see equation 8 in Bond et al. 2010), v_Φ, on distance from the Galactic plane, $|Z|$, for 14,000 high-metallicity ($[Fe/H] > -0.9$; panel *a*) and 23,000 low-metallicity ($[Fe/H] < -1.1$; panel *b*) stars with $|b| > 80°$. In panels *a* and *b*, individual stars are plotted as small dots, and the medians in bins of $|Z|$ are plotted as large symbols. The 2-σ envelope around the medians is shown by heavy gray dashed lines. The bottom two panels compare the medians (*c*) and dispersions (*d*) for the two subsamples shown in the top panels, and the dashed lines in the bottom two panels show predictions of a kinematic model from Bond et al. (2010). The light gray dotted lines in panel *d* show model dispersions (without correction for measurement errors). Reprinted from Bond et al. (2010).

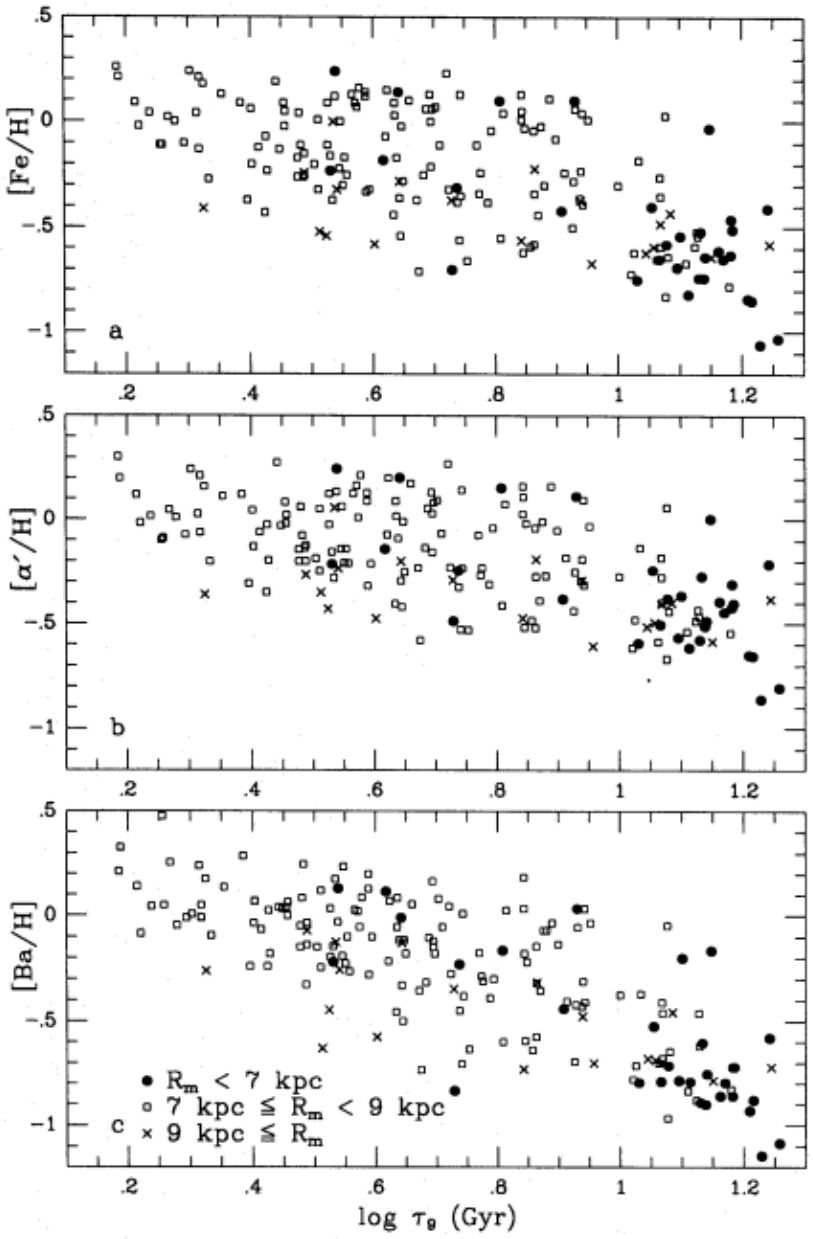

Fig. 14a–c. The abundances of iron **a**, α'-elements (the mean of the logarithmic silicon and calcium abundances) **b** and barium **c** as a function of logarithmic age. The symbols identify stars of different R_m

Edvardsson et al 1993

Galactic F & G Disk Stars in the Solar Neighborhood

Globular Clusters in the Galaxy

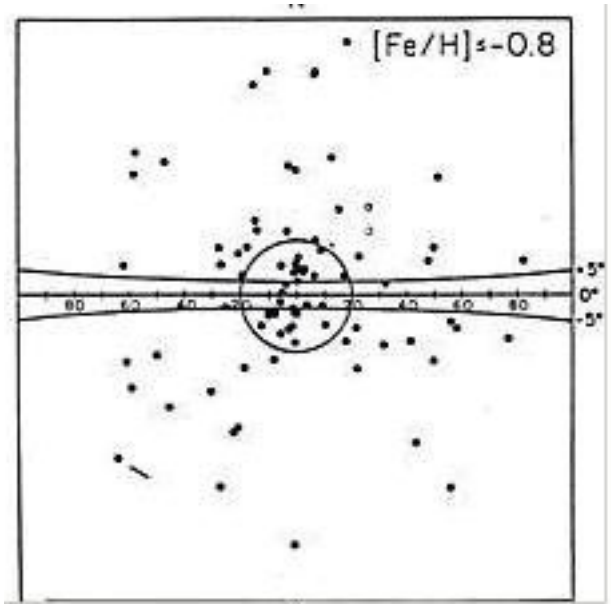

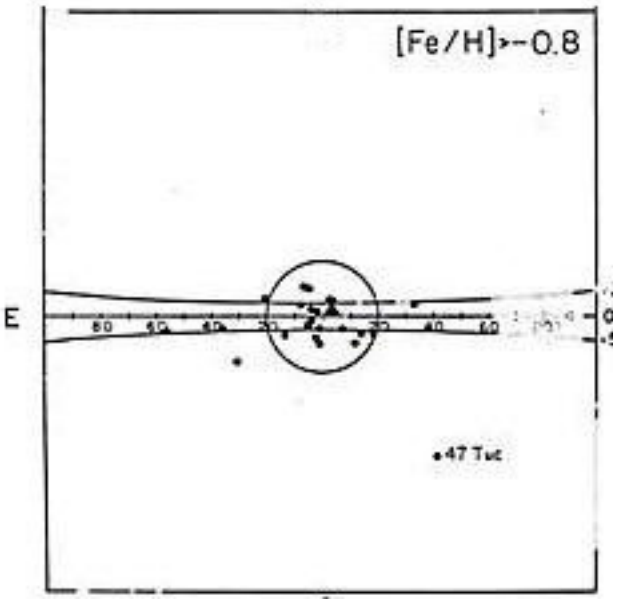

Zinn+1985

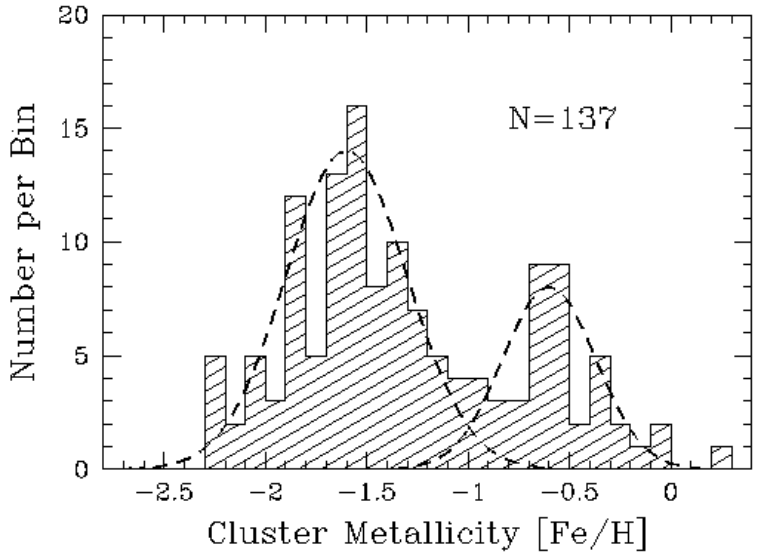

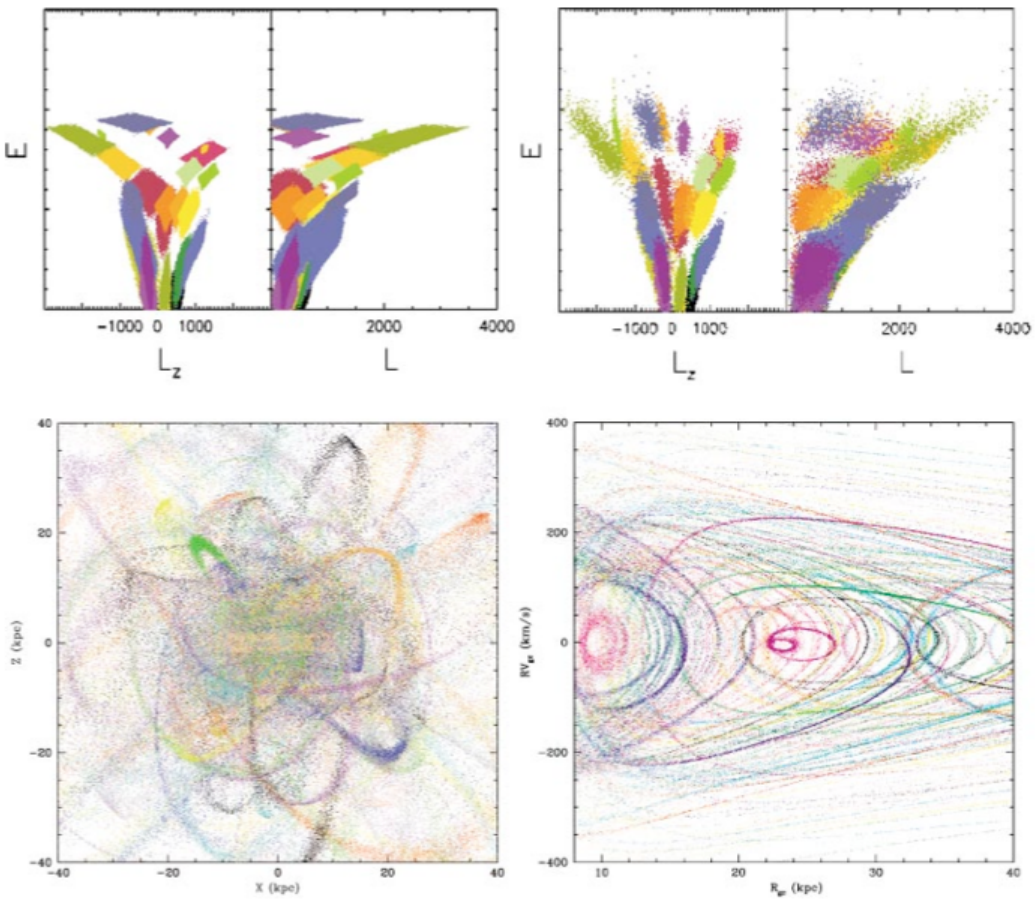

Figure 10 (*a*) Initial distribution of particles for 33 systems falling into the Galactic halo in integral of motion space. (*b*) The final distribution of particles in (*a*) after 12 Ga; the data points have been convolved with the errors expected for Gaia. [We acknowledge A. Helmi for these images.] (*c*) A simulation of the baryon halo built up through accretion of 100 satellite galaxies. The different colors show the disrupted remnants of individual satellites. (*d*) This is the same simulation shown in a different coordinate frame, i.e., the orbit radius (horizontal) plotted against the observed radial velocity (vertical) of the star. [We acknowledge P. Harding and H. Morrison for these images.]

Freeman and Bland-Hawthorn 2002, ARAA

Model of the Sagittarius Dwarf Stream
(Law et al 2005)

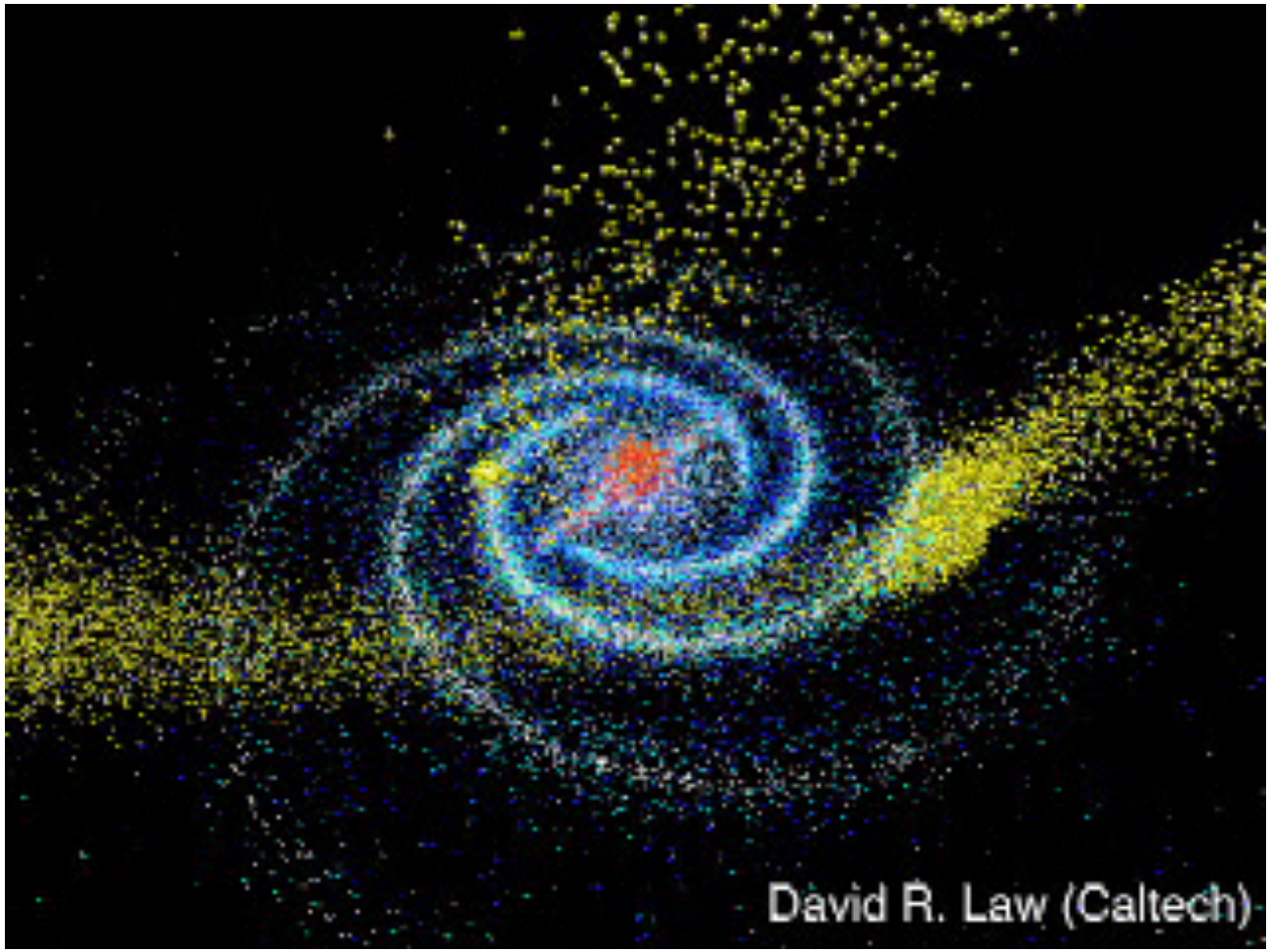

10 deg ~ 1.5 kpc at the Galactic Center

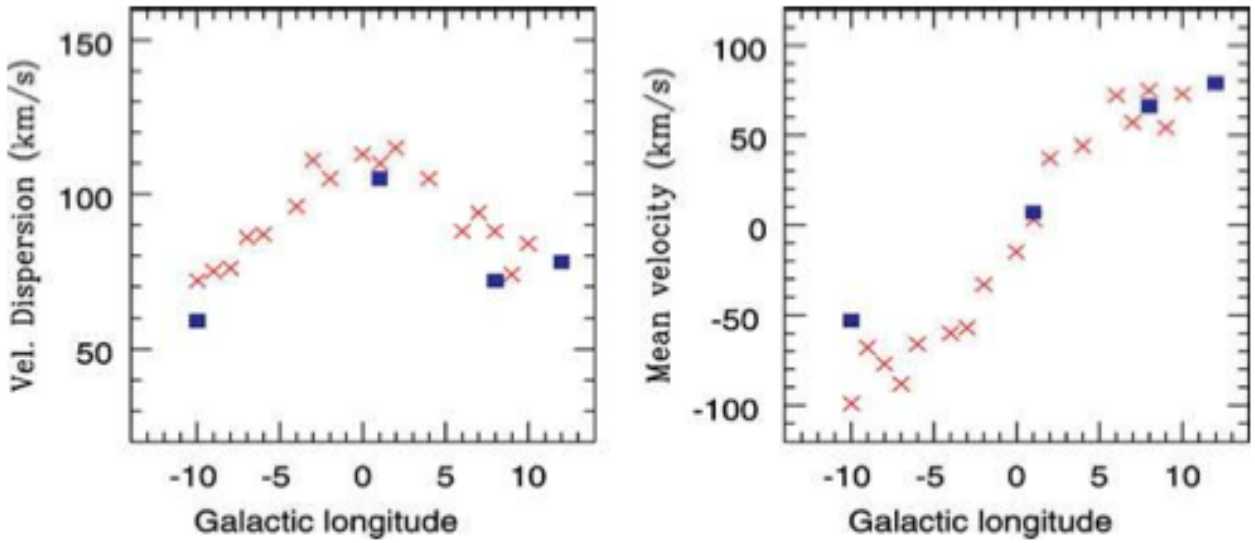

Figure 3. Bulge rotation from radial velocities of K-giants as measured by Minniti (1996), compared with the measurements of M-giants by Rich *et al.* (2007) (crosses). The latter have been corrected for the Solar motion around the Galaxy, which was not taken into account in the original paper.

v_{rot} ~75 km/s
$\sigma \cong 110$ km/s
$v_{rot}/\sigma \cong 0.67$

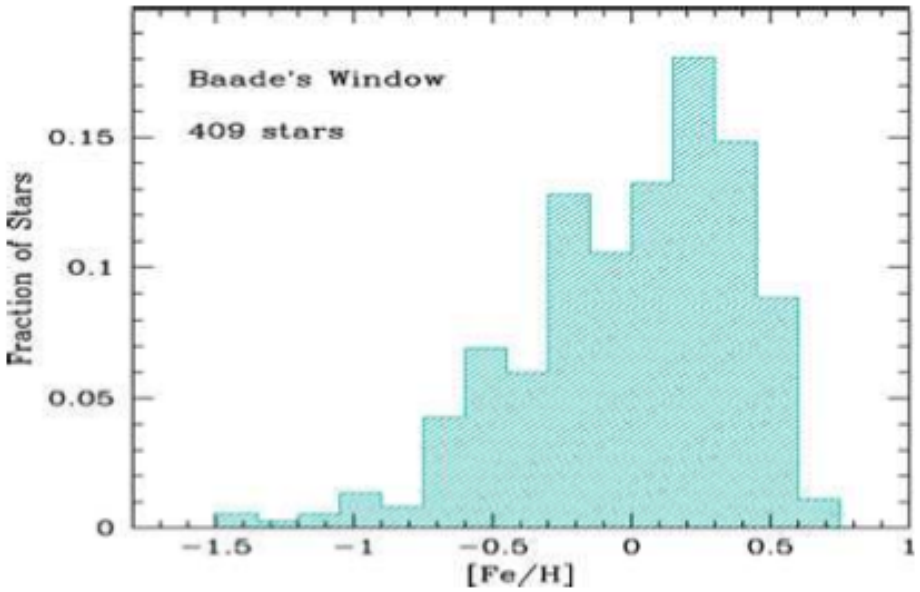

Figure 6. Metallicity distribution of 409 RGB and clump K-giants in the bulge from Zoccali *et al.* (2007) and Lecureur *et al.* (2007b), all measured for the first time with high-resolution spectra. This is in a firm metallicity scale as they observed simultaneously a dozen stars of known globular clusters located in the bulge.

The bulge of the MW is metal-rich but OLD

Green= bulge
Blue = thick disk
Red = thin disk

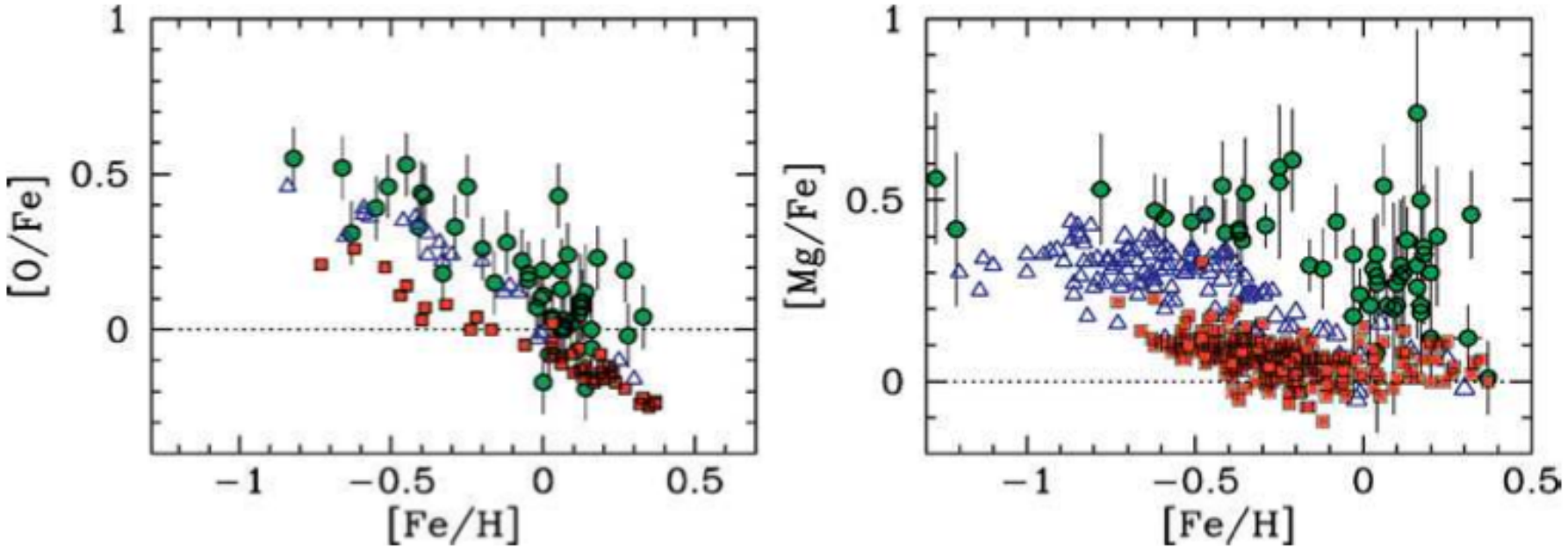

Figure 7. Oxygen and magnesium over iron ratios as measured from high dispersion spectra of bulge K giants (Zoccali et al. 2007, Lecureur *et al.* 2007a). Green circles with error bars are bulge stars, compared with thick (blue triangles) and thin (red squares) disk stars. These results clearly indicate that the bulge formed as a separate component by a rapid chemical enrichment.